The Journal of **Immunology**

Phosphatidylinositol 4-Phosphate 5-Kinase β Controls Recruitment of Lipid Rafts into the Immunological Synapse

Marinos Kallikourdis, Anna Elisa Trovato, Giuliana Roselli, Michela Muscolini, Nicla Porciello, Loretta Tuosto and Antonella Viola

---

Supplementary Material	http://www.jimmunol.org/content/suppl/2016/01/15/jimmunol.1501788.DCSupplemental.html
References	This article **cites 54 articles**, 24 of which you can access for free at: http://www.jimmunol.org/content/196/4/1955.full#ref-list-1
Subscriptions	Information about subscribing to *The Journal of Immunology* is online at: http://jimmunol.org/subscriptions
Permissions	Submit copyright permission requests at: http://www.aai.org/ji/copyright.html
Email Alerts	Receive free email-alerts when new articles cite this article. Sign up at: http://jimmunol.org/cgi/alerts/etoc

---

Phosphatidylinositol 4-Phosphate 5-Kinase β Controls Recruitment of Lipid Rafts into the Immunological Synapse

Marinos Kallikourdis,[*,†] **Anna Elisa Trovato,**[†] **Giuliana Roselli,**[†] **Michela Muscolini,**[‡] **Nicla Porciello,**[‡] **Loretta Tuosto,**[‡] **and Antonella Viola**[§]

Phosphatidylinositol 4,5-biphosphate (PIP2) is critical for T lymphocyte activation serving as a substrate for the generation of second messengers and the remodeling of actin cytoskeleton necessary for the clustering of lipid rafts, TCR, and costimulatory receptors toward the T:APC interface. Spatiotemporal analysis of PIP2 synthesis in T lymphocytes suggested that distinct isoforms of the main PIP2-generating enzyme, phosphatidylinositol 4-phosphate 5-kinase (PIP5K), play a differential role on the basis of their distinct localization. In this study, we analyze the contribution of PIP5Kβ to T cell activation and show that CD28 induces the recruitment of PIP5Kβ to the immunological synapse, where it regulates filamin A and lipid raft accumulation, as well as T cell activation, in a nonredundant manner. Finally, we found that Vav1 and the C-terminal 83 aa of PIP5Kβ are pivotal for the PIP5Kβ regulatory functions in response to CD28 stimulation. *The Journal of Immunology*, 2016, 196: 1955–1963.

Phosphatidylinositol 4,5-biphosphate (PIP2) represents <1% of the inner leaflet plasma membrane phospholipids and occupies a pivotal role in several signaling processes (1, 2). In T lymphocytes, PIP2 serves as a precursor for second messengers inositol triphosphate, diacylglycerol, and phosphatidylinositol 3,4,5-triphosphate, which are generated by two major distinct signaling cascades involving phospholipase Cγ1 (3) and PI3K (4), respectively. In addition, PIP2 itself functions as a signaling molecule by directly associating several intracellular proteins and modulating their subcellular localization or activity, including actin-binding proteins (5), such as talin, vinculin, and filamin (6, 7). Indeed, PIP2 accomplishes an important role as a regulator of cytoskeletal dynamics and, often in concert with small GTPases, controls cell shape, endo- and exocytosis, cell migration, and cell–cell adhesion (1).

Both lymphocyte migration and activation require the compartmentalization of membrane receptors and signaling molecules in specific cell locations. Lymphocyte polarization is accompanied by rapid cytoskeletal reorganization and, at the plasma membrane, by the assembly of membrane lipid rafts (8). In T lymphocytes, the engagement of the costimulatory molecule CD28 at the immu-

nological synapse (IS) promotes the organization of a signaling compartment by inducing cytoskeletal rearrangements and lipid raft accumulation (9–11). All these events are necessary for enhancing TCR-controlled signaling pathways (11–13). CD28 also recruits filamin A (FLNA), which in turn cooperates with the Vav-dependent actin polymerization pathway to induce lipid raft accumulation at the IS (14). In addition to initiating and sustaining TCR-dependent signal transduction (10), lipid rafts constitute a dynamic signaling platform for PIP2, by providing a specialized lipid environment where critical signaling proteins accumulate (15). Approximately half of the PIP2 content within the cell is synthesized preferentially in these cholesterol/sphingolipid-enriched membrane domains (16), which exhibit locally regulated PIP2 turnover and restricted diffusion-mediated exchanges with their environment (17).

The main pathway of PIP2 synthesis involves phosphorylation of phosphatidylinositol 4-phosphate on the D-5 position of the inositol ring by type I phosphatidylinositol 4-phosphate 5-kinases (PIP5K) (18). Primary CD4^{+} T cells express all three PIP5K isoforms (α, β, and γ), with a specific subcellular localization (19). Human PIP5Kα accumulates in a sustained manner in the T:APC contact zone (20), where it regulates CD28-mediated actin polymerization events necessary for CD28 costimulatory signaling (21, 22). PIP5Kγ90 is predominantly found at the distal pole and in the uropod. PIP5Kβ and PIP5Kγ87 are rapidly but transiently recruited to the site of T:APC contacts during IS formation (20). PIP5Kγ87 has been implicated in the formation of a stable T:APC interaction by regulating the transition of LFA-1 from a low intermediate to a high-activation state (23). Less is known about the role of PIP5Kβ at the IS in T lymphocytes.

Data from other cell types suggest that PIP5Kβ is targeted to the plasma membrane and/or activated when overexpressed (24–26). Overexpression of PIP5Kβ induces actin polymerization (27–30) and actin comets from lipid rafts at the plasma membrane (31). In B cells, PIP5Kβ is recruited to lipid rafts during cell triggering (32).

In this study, we provide evidence that PIP5Kβ is recruited into the IS, in a CD28- and Vav1- dependent manner. In the IS, PIP5Kβ regulates actin reorganization events that are required for lipid raft recruitment. Finally, we identified the 83 C-terminal amino acids of PIP5Kβ as the key domain required for these regulatory functions.

*Humanitas University, Rozzano, Milan 20089, Italy; †Adaptive Immunity Laboratory, Humanitas Clinical and Research Center, Rozzano, Milan 20089, Italy; ‡Pasteur Institute–Cenci Bolognetti Foundation, Department of Biology and Biotechnology Charles Darwin, Sapienza University, 00185 Rome, Italy; and §Department of Biomedical Sciences, University of Padua and Venetian Institute of Molecular Medicine, 35131 Padua, Italy

ORCID: 0000-0001-9318-3368 (M.K.).

Address correspondence and reprint requests to Prof. Loretta Tuosto, Department of Biology and Biotechnology Charles Darwin, Sapienza University, Via dei Sardi 70, 00185 Rome, Italy. E-mail address: loretta.tuosto@uniroma1.it

The online version of this article contains supplemental material.

Abbreviations used in this article: DIC, differential interference contrast; EGFP, enhanced GFP; FLNA, filamin A; IS, immunological synapse; MFI, mean fluorescence intensity; PIP2, phosphatidylinositol 4,5-biphosphate; PIP5K, phosphatidylinositol 4-phosphate 5-kinase; ROI, region of interest; WT, wild type.

Materials and Methods

Cells, reagents, and Abs

The Jurkat T cell line J.E6-1 (purchased from the American Type Culture Collection), the EBV-B 221 cell line, and primary resting human peripheral blood CD4^{+} T cells were cultured in RPMI 1640 medium (Lonza) with 10% heat-inactivated bovine serum, 2 mM L-glutamine, sodium pyruvate, and nonessential amino acids. Primary CD4^{+} T cells were isolated from buffy coats by negative selection using CD4 RosetteSep (StemCell Technologies). The Vav1-deficient Jurkat cell line J.Vav1 and a J.Vav1 derivative cell line, J.Vav1.WT, stably re-expressing Vav1, were maintained as above with the addition of 0.5 mg/ml G418 (33). Murine L cells Dap3, transfected with human B7.1/CD80 (Dap3/B7) or HLA-DRB1*0101 (5-3.1) or 5-3.1, cotransfected with B7.1/CD80 (5-3.1/B7), were previously described (12, 34). EBV-B cells, Dap3 cells, and 5-3.1 fibroblasts were used as APCs in T:APC conjugate formation experiments.

The following Abs were used: mouse anti-hemagglutinin (F7) and rabbit anti-hemagglutinin (Y11); mouse anti-CD28.2, mouse anti-CD3 (UCHT1), and goat anti-mouse (BD Biosciences); mouse anti-myc (9E10) (Roche); mouse anti-FLAG (M2) (Sigma-Aldrich); and sheep anti–SLP-76 and mouse anti-phosphotyrosine (4G10) (Millipore).

Plasmids, transfections, and luciferase assays

Enhanced GFP (EGFP)-PIP5Kβ, EGFP-PIP5Kβ[K138A], and EGFP-PIP5KβΔ456 constructs were gifts of R. Lacalle and S. Manes (Consejo Superior de Investigaciones Cientificas). MyrPalm-mCFP was a gift of R. Tsien (Howard Hughes Medical Institute, San Diego, CA). Primary CD4^{+} T cells were transfected using an Amaxa electroporator. Jurkat T cells were transfected using a Bio-Rad electroporator. pEF-*Bos* expressing C-terminal myc-tagged Vav1 was previously described (34). FLAG-tagged SLP-76 wild type (WT) was provided by G. Koretzky (Weill Cornell Medical College, New York, NY).

The NF-AT luciferase reporter construct containing the luciferase gene under the control of the human IL-2 promoter NF-AT binding site was provided by C. Baldari (University of Siena, Siena, Italy). For luciferase assays, 10^7 Jurkat cells were electroporated (at 260 V, 960 μF) in 0.5 ml RPMI 1640 supplemented with 20% FCS with 10 μg NF-AT luciferase together with 5 μg pEGFP and 20 μg each indicated expression vector, keeping the total amount of DNA constant (40 μg) with empty vector. Twenty-four hours after transfection, cells were stimulated with 5-3.1 or 5-3.1/B7 cells prepulsed at 37°C for 6 h. Luciferase activity was measured according to the manufacturer's instruction (Promega). Luciferase activity was determined in triplicates after normalization to GFP values.

T:APC conjugate formation for confocal microscopy experiments

For experiments with human primary resting CD4^{+} T cells, APC were resuspended at 10^7 cells/ml and incubated (or not) with 1 μg/ml bacterial superantigens SEA, SEB, and SEE (Toxin Technology) at 37°C for 2 h. For experiments with Jurkat T cells, only 1 μg/ml SEE was used to load APCs. APCs were then washed and incubated at 37°C for 15 min with equal number of Jurkat T cells or with twice as many primary resting human CD4^{+} T cells. Cells were allowed to adhere to microscope slides coated with 0.05 mg/ml poly-L-lysine, fixed with 4% paraformaldehyde, washed, and either permeabilized with 0.1% Triton/PBS and stained with primary and secondary reagents, or directly mounted with vectashield mounting medium, with or without DAPI (Vector Laboratories). Images were acquired with fine focusing oil immersion lens (×60, NA 1.35) using a FV1000 laser-scanning confocal microscope (Olympus). Differential interference contrast (DIC; Nomarski technique) was also acquired.

Measurement of conjugate formation

Conjugate formation was measured, as previously described (22). Briefly, Jurkat J.E6-1 cells were transfected with EGFP-PIP5Kβ or EGFP-PIP5KβΔ456 constructs and transfectants (10^7/ml) were incubated for 15 min at 37°C, with CMTMR-stained 5-3.1/B7 cells (2.5×10^6/ml) in a final volume of 100 μl RPMI 1640, then diluted with an additional 100 μl RPMI 1640 and analyzed by FACS. Conjugates were identified as EGFP[+] CMTMR^{+} cells and expressed as mean percentage ± SEM out of transfected cells.

Image analysis

Acquired images were analyzed on Image J. To quantify the recruitment to the IS, regions of interest (ROIs) were drawn around the immunological synapse (ROI$_{IS}$) and around the rest of the cell membrane (ROI$_{non-IS}$) of the T cell. A ROI was also drawn in a background area outside the cell. The relative recruitment index was calculated as indicated: (mean fluorescence intensity [MFI] in the ROI$_{IS}$ − MFI of background)/(MFI in the ROI$_{non-IS}$ − MFI of background). The raw relative recruitment index values were plotted for all experiments. Signal intensity was calculated on Image J using the multimeasure function. Morphological analysis was performed on Imaris (Bitplane).

Measurement of F-actin content

EGFP-PIP5Kβ– or EGFP-PIP5KβΔ456–transfected primary human CD4^{+} T cells were transferred to Eppendorf tubes (on ice), where 1 μg/ml anti-CD3 (eBio) and 10 μg/ml anti-CD28 (BD Biosciences) were administered, followed by cross-linking with 5 μg/ml anti-mouse IgG (Southern Bio), while maintaining all reagents and cells on ice. Activation was performed by bringing the mixture to 37°C for 5 min, by placing the tubes in pre-heated damp tissues in a 37°C incubator, prior to returning on ice for fixation, permeabilization, and phalloidin staining, which was analyzed by flow cytometry.

RNA interference, real-time PCR, and T cell activation assay

Primary human CD4^{+} T cells were transfected with 5 μg small interfering RNAs specific for PIP5Kβ (siGENOME human PIP5K1B-8395-small interfering RNA, clone 03; Thermo Scientific) or with 5 μg scrambled control, using Amaxa Nucleofector kit. Cells were then incubated in RPMI 1640 medium for 48 h before harvesting for use in activation experiments and mRNA quantification. T cells were activated with anti-CD3 (2 μg/ml) and anti-CD28 (1 μg/ml). Cells were analyzed for CD69 and CD25 expression 12 h after activation by FACS, using anti-CD25 and anti-CD69 directly conjugated Abs (BD Biosciences). RNA extraction was performed using RNeasy micro kit (Qiagen). cDNA was prepared using High-Capacity cDNA Reverse Transcription Kit (Applied Biosystems). Real-time PCR was performed using TaqMan assays for PIP5Kβ and 18S rRNA and Real-Time PCR Master mix and performed using the ABI PRISM 7900 Sequence Detection System (Applied Biosystems).

Measurement of intracellular calcium concentration

Primary human CD4^{+} T cells (1.5×10^6/ml) were loaded with 20 μM Fluo-3 AM (Sigma-Aldrich) for 30 min at 37°C in 400 μl buffer containing 125 mM NaCl, 5 mM KCl, 1 mM Na$_2$HPO$_4$, 1mM CaCl$_2$, 0,5 mM MgCl$_2$, 1 mg/ml glucose, and 50 mM HEPES. Loaded cells were then incubated with 5 ml same buffer for 20 min, washed, and activated with anti-CD3 (5 μg/ml) plus anti-CD28 (5 μg/ml) Abs cross-linked with anti-mouse IgG (10 μg/ml) at 37°C, and immediately analyzed by a cytofluorimeter (FACSCalibur; BD Biosciences). Changes in cell fluorescence were monitored every 24 s for 10 min by measuring fluorescence emission at 530 nm. The concentration of intracellular calcium was calculated according to Grynkiewicz et al. (35). The following Abs were used: mouse anti-CD28.2, mouse anti-CD3 (UCHT1), and goat anti-mouse IgG (BD Biosciences, Milan, Italy).

Statistical analysis

Statistical analysis was performed with GraphPad Prism software, using unpaired *t* test for Gaussian or Mann–Whitney *U* test for non-Gaussian distributions, after normality testing. Multiple comparisons were analyzed using one-way ANOVA.

Results

PIP5Kβ is recruited into the IS in a CD28-dependent manner

To address the relevance of PIP5Kβ in T cell activation, human primary CD4^{+} T cells were transfected with EGFP-PIP5Kβ WT and stimulated for 15 min with EBV-B cells unpulsed or pulsed with a mixture of superantigens. Confocal microscopy analyses showed that PIP5Kβ was recruited to the plasma membrane at the T:APC interface, both when unpulsed or superantigen-pulsed APC were used (Fig. 1A). These data suggest that molecules other than TCR are responsible for the recruitment of PIP5Kβ to the membrane at the T:APC interface.

CD28 represents a key node in the regulation of PIP2 turnover by recruiting and activating PIP5Kα (21, 22). To verify whether CD28 was also involved in PIP5Kβ recruitment, Jurkat cells
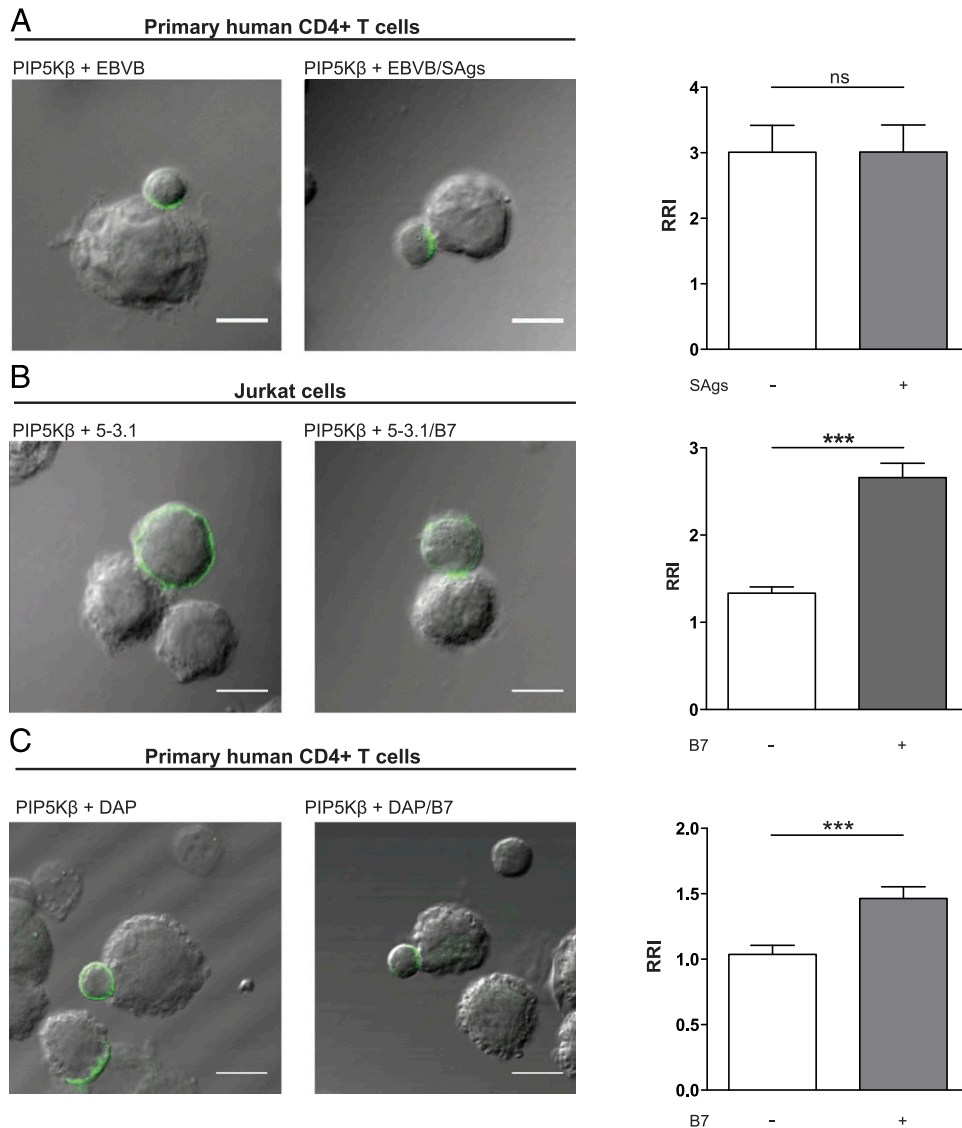
FIGURE 1. CD28 mediates PIP5Kβ recruitment into the IS independently of TCR engagement. (**A**) Primary human CD4^{+} T cells transfected with EGFP-PIPKβ plasmid were incubated with EBV-B cells pulsed with a mixture of superantigen (sAg) (SEA, SEB, SEE) (gray bars) or unpulsed (white bars) for 15 min. Conjugates were allowed to adhere on slides and subsequently fixed. EGFP-PIP5Kβ recruitment to the IS was evaluated by confocal microscopy. Representative overlapped fluorescence and DIC images are shown (EGFP signal shown in green). Graphs show the quantitative analysis of PIP5Kβ recruitment at the IS. RRI was calculated as described in *Materials and Methods*. Nonparametric *t* test was performed. Bars show mean RRI values ± SEM from 33 (PIP5Kβ + EBVB) and 30 (PIP5Kβ + EBVB/sAg) conjugates. (**B**) JE6.1 Jurkat T cells, transfected with EGFP-PIP5Kβ plasmid, were incubated with L-cell 5-3.1 fibroblasts, expressing (gray bars) or not (white bars) human B7-1, for 15 min. Representative confocal images and quantitative analysis of EGFP-PIP5Kβ RRI to the IS are shown. Nonparametric *t* test was performed. Bars show mean RRI values ± SEM from 61 (PIP5Kβ + 5-3.1) and 89 (PIP5Kβ + 5-3.1/B7) conjugates, from four independent experiments. (**C**) Primary human CD4^{+} T cells transfected with EGFP-PIPKβ were incubated with Dap3 cells expressing (gray bars) or not (white bars) human B7-1. Graph shows the quantitative analysis of PIP5Kβ RRI to the IS. Bars show mean RRI values ± SEM from 21 (PIP5Kβ + Dap3) and 35 (PIP5Kβ + Dap3/B7) conjugates, from two independent experiments. Scale bar, 10 μm. Nonparametric *t* test was performed. ****p* < 0.001.

(Fig. 1B) and primary T cells (Fig. 1C) transfected with EGFP-PIP5Kβ WT were stimulated with murine fibroblasts stably transfected with or without human B7.1, the ligand for CD28. The conjugation of PIP5Kβ WT-transfected Jurkat cells with 5-3.1/B7 APC was sufficient to determine PIP5Kβ WT recruitment to the T:APC contact site (Fig. 1B). The same result was obtained by conjugation of PIP5Kβ WT-transfected primary T cells with Dap3/B7 cells, even though the latter lack the expression of a functional human HLA molecule. In addition, PIP5Kβ was not recruited in either Jurkat (Fig. 1B) or primary T cells conjugated with cells lacking B7 expression (Fig. 1C). The representative fluorescence and DIC images are shown in Supplemental Fig. 4A–C.

Thus, similarly to what has been observed for PIP5Kα (21, 22), CD28 mediates the membrane recruitment of PIP5Kβ in a TCR-independent manner.

The C-terminal domain of PIP5Kβ is required for its accumulation at the IS

To analyze the molecular determinants of PIP5Kβ recruitment to the IS, we used the dominant-negative mutant of PIP5Kβ Δ456, which retains its kinase activity, but lacks the last 83 aa (36). In Jurkat cells, CD28-mediated recruitment of PIP5Kβ Δ456 mutant to the T:APC interface was strongly impaired (Fig. 2A). The representative fluorescence and DIC images are shown in Supplemental Fig. 4C. Similar results were obtained by confocal

microscopy analysis performed on primary CD4^{+} T cells (Supplemental Fig. 1). In contrast to what has been observed for PIP5Kα (22), the lipid kinase activity of PIP5Kβ was dispensable for PIP5Kβ recruitment to the IS in response to CD28 stimulation, as demonstrated by expressing the K138A kinase-dead mutant of PIP5Kβ (37) in Jurkat cells (Supplemental Fig. 2A).

We have recently demonstrated that CD28-mediated recruitment of PIP5Kα to the T:APC interface is essential for CD28-mediated actin polymerization; we identified Vav1, a guanine-nucleotide exchange factor for Rac1 and Cdc42 GTPases (38), as the linker molecule that couples CD28 to the recruitment and activation of PIP5Kα (22). To assess the role of Vav1 in CD28-mediated recruitment of PIP5Kβ, we used Vav1-deficient Jurkat T cells (J.Vav1) and J.Vav1 cells stably reconstituted with human

Vav1 (JVav.1.VavWT). In the absence of Vav1, PIP5Kβ recruitment to the T:APC interface was strongly impaired in CD28-stimulated cells (Fig. 2B). The representative fluorescence and DIC images are shown in Supplemental Fig. 4D. Consistently with the data obtained for PIP5Kα (22), PIP5Kβ is also constitutively associated with Vav1 when coexpressed in Jurkat cells (Fig. 2C).

To verify whether PIP5Kβ acts downstream of Vav1, as observed for PIP5Kα (22), we looked at NF-AT activation, an event that we have previously demonstrated to depend on both Vav1 (34) and PIP5Kα (21). As already described (34), overexpression of Vav1 induced NF-AT–dependent transcription following CD28 engagement in the absence of TCR engagement. The expression of PIP5KβΔ456 dominant-negative mutant strongly impaired
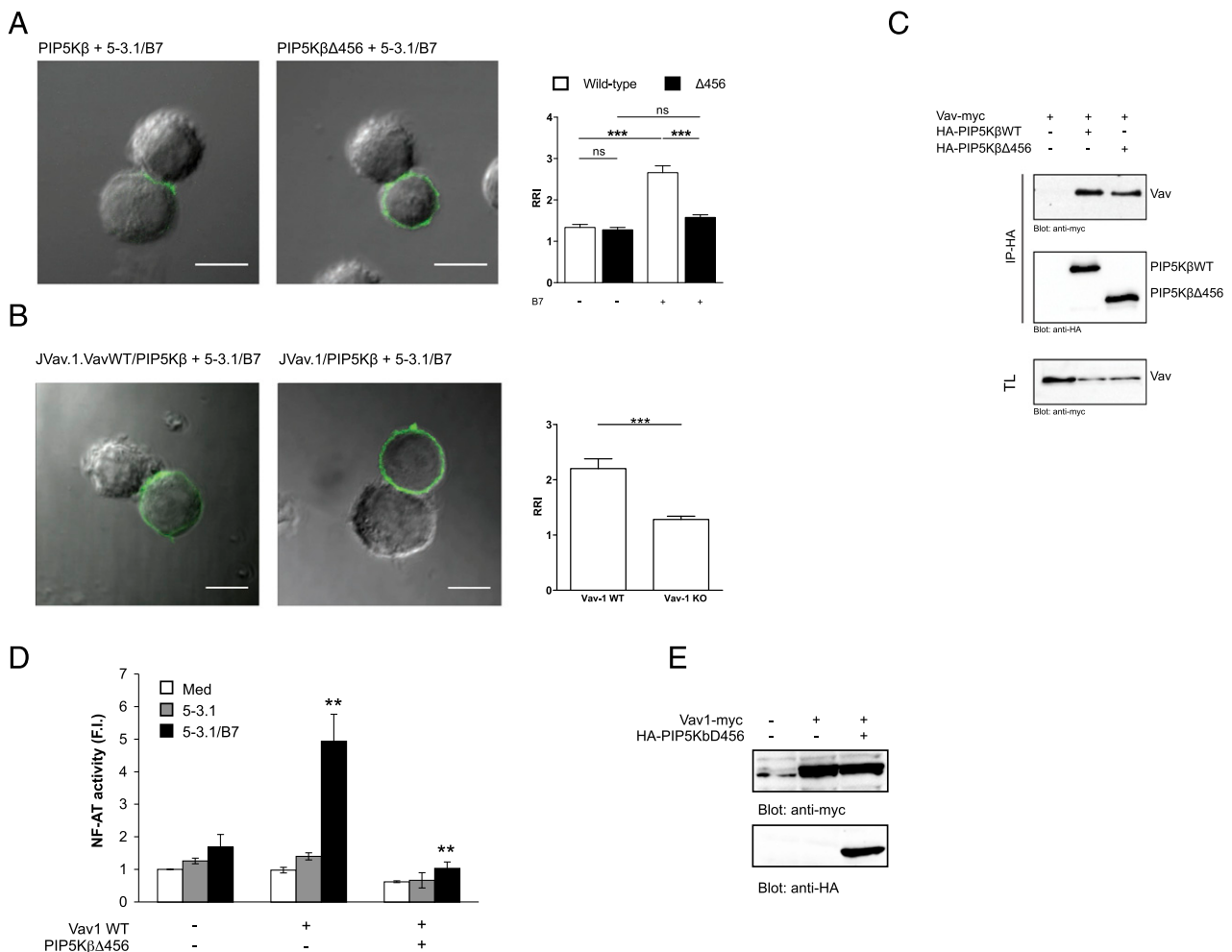

FIGURE 2. The C-terminal domain of PIP5Kβ and Vav1 is required for PIP5Kβ recruitment into the IS. (**A**) JE6.1 Jurkat T cells, transfected with EGFP-PIPKβ (white bars) or EGFP-PIPKβΔ456 (black bars), were incubated with 5-3.1 fibroblasts, expressing or not human B7-1 (B7), for 15 min. Graph shows the quantitative analysis of PIP5Kβ and PIPKβΔ456 RRI to the IS. Bars show mean RRI values ± SEM from 61 (PIP5Kβ + 5-3.1), 61 (PIP5KβΔ456 + 5-3.1), 89 (PIP5Kβ + 5-3.1/B7), and 79 (PIP5KβΔ456 + 5-3.1B7) conjugates, from four independent experiments. Nonparametric one-way ANOVA test was performed. ***$p < 0.001$. (**B**) JE6.1 Jurkat T cells, expressing Vav1 WT (JVav.1.VavWT) or deficient for Vav1 (JVav.1), and transfected with EGFP-PIP5Kβ, were allowed to form conjugates with unpulsed 5-3.1 fibroblasts expressing B7-1 for 15 min. Representative confocal images and quantitative analysis of EGFP-PIP5Kβ RRI to the IS are shown. Scale bar, 10 μm. Bars show mean RRI values ± SEM from 30 (J.Vav1.VavWT + 5-3.1/B7) and 32 (J.Vav1 + 5-3.1/B7) conjugates, from the summary of two independent experiments. Nonparametric t test was performed. ***$p < 0.001$. (**C**) Jurkat cells were transfected with Vav-myc alone or in combination of HA-PIP5KβWT or HA-PIP5KβΔ456 expression vectors. Anti-hemagglutinin immunoprecipitations (IP) were performed on cellular extracts, and anti-myc (*upper* and *middle panels*) or anti-hemagglutinin (*middle panel*) Western blots were performed on either IP or total lysates (TL). (**D**) NF-AT luciferase activity of Jurkat cells transfected with empty vector (−) or Vav1 WT alone or in combination with hemagglutinin-PIP5Kβ Δ456 mutant and stimulated in the absence (med) or presence of B7-negative (5-3.1) or 5-3.1/B7 cells. Data are expressed as F.I. over the basal level of cells transfected with empty vector (−) and unstimulated (med), after normalization to GFP values. Bars show mean ± SEM of one experiment representative of three. Asterisks (*) indicate $p < 0.05$ calculated by Student t test. (**E**) The expressions of myc-Vav1 (*upper panel*) and HA-PIP5Kα K182A (*lower panel*) were analyzed by Western blotting. All data are representative of three independent experiments.

Vav1-mediated NF-AT activation in CD28-stimulated cells (Fig. 2D). Finally, overexpression of the PIP5Kβ∆456 dominant-negative mutant did not modify the tyrosine phosphorylation Vav or SLP-76 induced by anti-CD3/anti-CD28 (Supplemental Fig. 3).

These data indicate that Vav1 is essential for PIP5Kβ recruitment to the membrane in response to CD28 stimulation and that PIP5Kβ acts downstream of Vav1.

The C-terminal domain of PIP5Kβ mediates cytoskeletal rearrangement and FLNA recruitment into the IS

Lymphocyte activation and polarization are accompanied by rapid cytoskeletal rearrangements and by the assembly of specialized membrane rafts. PIP5Kβ has a major role in actin rearrangement events regulating several cell functions, including uropod retraction (36) and the formation of motile actin comets (31), stress fibers (30), and membrane ruffling (24). Human primary CD4^{+} T cells expressing EGFP-PIP5Kβ WT or ∆456 mutant were activated with anti-CD3 plus anti-CD28 Abs, and F-actin accumulation, spreading, and podia formation were analyzed. A strong increase of F-actin content was observed in PIP5Kβ WT-expressing cells, after stimulation with anti-CD3 plus anti-CD28 Abs. By contrast, the overexpression of PIP5Kβ ∆456 mutant significantly impaired the accumulation of F-actin in anti-CD3–plus anti-CD28–stimulated cells (Fig. 3A). In addition, PIP5Kβ ∆456-expressing cells were characterized by impaired formation of protruding podia (Fig. 3B) and reduced cell perimeter (Fig. 3C) compared with PIP5Kβ WT-expressing cells, and retained a more evident circular shape after stimulation (Fig. 3D). The representative fluorescence and DIC images are shown in Supplemental Fig. 4F. Altogether, these results showed a pivotal role of the C-terminal tail of PIP5Kβ in regulating actin remodeling upon T cell activation.

Actin polymerization at the IS is regulated by Vav1, the Wiscott–Aldrich syndrome protein, and the ARP2/3 complex. The ARP2/3 complex cooperates with the actin–cross-linking proteins filamins to generate and maintain the cortical actin cytoskeleton (39). FLNA is the form of filamin predominantly expressed in the immune system (40). We have previously demonstrated that CD28 recruits FLNA into the IS (14), where FLNA organizes TCR (41) and CD28 (14) signaling. In PIP5Kβ ∆456-expressing Jurkat cells, FLNA recruitment was strongly impaired (Fig. 3E). The representative fluorescence and DIC images are shown in Supplemental Fig. 4E. On the contrary, the lipid kinase activity of PIP5Kβ was not required for FLNA recruitment to the IS (Supplemental Fig. 2B).

The C-terminal domain of PIP5Kβ mediates membrane raft recruitment into the IS, thus affecting T cell activation

Lipid rafts constitute a dynamic signaling platform by providing initiation, spatial regulation, and sustenance of TCR-dependent
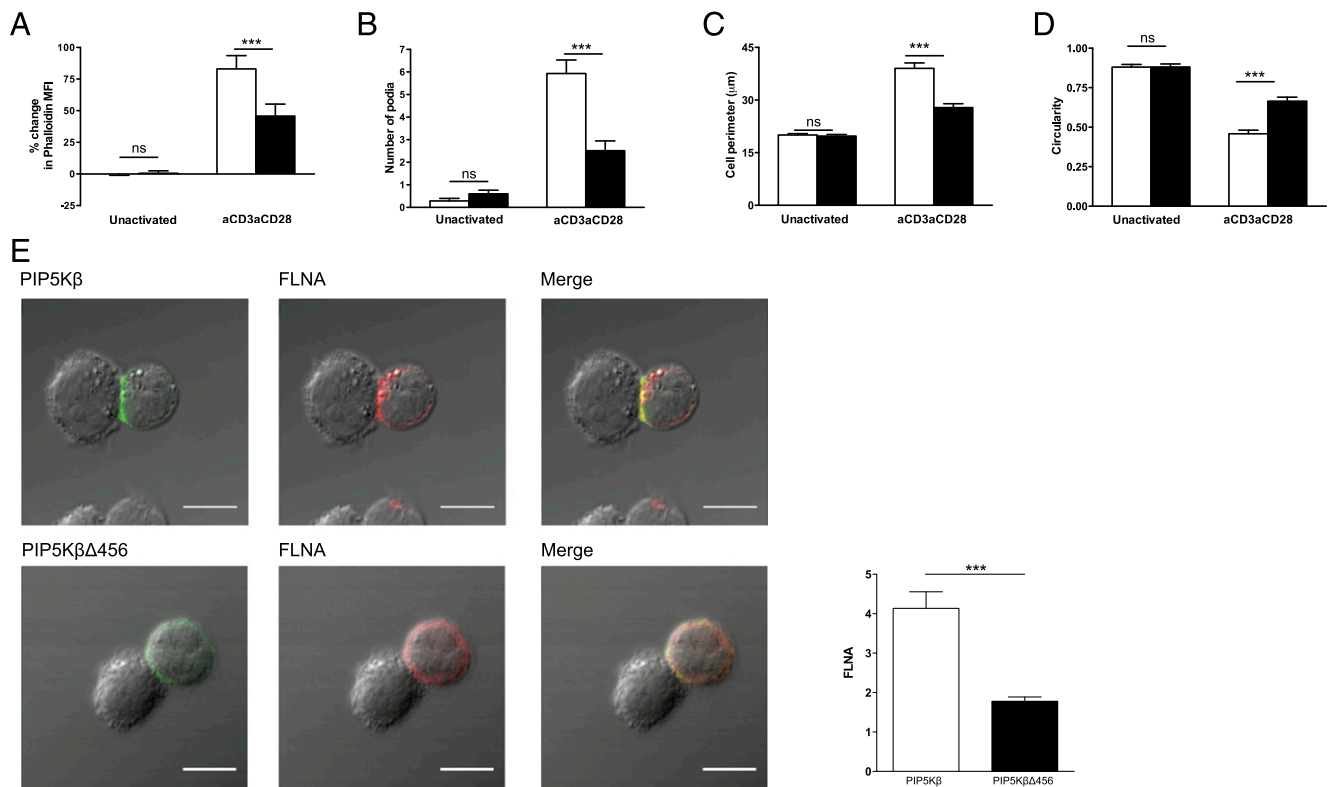

FIGURE 3. The C-terminal domain of PIP5Kβ is required for TCR/CD28-induced cytoskeleton rearrangements events. (A) Primary human CD4^{+} T cells were transfected with either PIP5Kβ (white bars) or PIP5Kβ∆456 (black bars). F-actin formation was evaluated by FACS 5 min after anti-CD3 and anti-CD28 stimulation with cross-linking. A two-way ANOVA test was applied. ***$p < 0.001$. (B–D) Primary human CD4^{+} T cells, transfected with either PIP5Kβ (white bars) or PIP5Kβ∆456 (black bars), were activated by anti-CD3 and anti-CD28 on glass slides. Number of podia (B), cell perimeter (C), and circularity (D) was evaluated 1 h after activation by confocal analysis. Quantitative analysis is shown. Bars show mean values ± SEM from 28 (Unactivated PIP5Kβ), 25 (PIP5Kβ + aCD3aCD28), 29 (Unactivated + PIP5Kβ∆456), and 37 (PIP5Kβ∆456 + aCD3aCD28) cells. The results represent the summary of two independent experiments. Two-way ANOVA with Bonferroni posttest was used. ***$p < 0.001$. (E) JE6.1 Jurkat T cells, transfected with EGFP-PIP5Kβ (white bars) or EGFP-PIP5Kβ∆456 (black bars), were allowed to form conjugates with SEE-pulsed 5-3.1 fibroblasts expressing B7-1. Representative confocal images of EGFP-PIP5Kβ (green) or EGFP-PIP5Kβ∆456 (green) and FLNA (red) are shown. The graph displays the quantitative analysis of FLNA RRI to the IS. Unpaired *t* test was used. ***$p < 0.001$. Scale bar, 10 μm. Bars show mean RRI values ± SEM from 74 (PIP5Kβ) and 55 (PIP5Kβ∆456) conjugates, from three independent experiments.

signal transduction. A significant pool of PIP2 associates with membrane rafts (16, 42), which exhibit locally regulated PIP2 turnover (17). Lipid raft assembly into the IS requires signaling through CD28 (9, 10, 14) and is regulated by FLNA (14). To verify a possible involvement of PIP5Kβ in raft accumulation, the lipid raft marker myr-palm-CFP was expressed in Jurkat T cells together with EGFP-PIP5Kβ WT or Δ456 mutant. Jurkat T cells, expressing either EGFP-PIP5Kβ WT or Δ456 mutant, were allowed to form conjugates with 5-3.1/B7 cells. Confocal microscopy analysis revealed that PIP5Kβ WT recruitment was accompanied by lipid raft polarization to the IS and that the expression of PIP5KβΔ456 mutant strongly inhibited raft recruitment to the T:APC contact zone (Fig. 4A) without affecting conjugate formation (Fig. 4C). Altogether, these data suggest that lack of PIP5Kβ recruitment to the IS affects the early signaling events regulating cytoskeletal rearrangements and membrane raft accumulation during T cell activation.

Raft accumulation at the IS is essential to amplify TCR signaling and provide CD28-mediated costimulatory signals (14); thus, the contribution of PIP5Kβ to T cell activation was evaluated. In primary T cells, efficient PIP5Kβ silencing (Fig. 5A) significantly impaired the increase of Ca^{2+} levels (Fig. 5B) as well as of CD69 (Fig. 5C) and CD25 expression (Fig. 5D) mediated by TCR and CD28 coengagement.

Altogether these data suggest a critical role played by PIP5Kβ in orchestrating the early cytoskeleton events necessary for the assembly of signaling complexes at the IS.

Discussion

Dynamic changes in the local availability of PIP2 at the plasma membrane regulate signaling, trafficking, and membrane-cytoskeleton linkage. In T lymphocytes, PIP2 concentrates at the IS at a very early stage upon Ag recognition (43), and data obtained by overexpressing PIP5K isoforms in transgenic mice showed the enrichment of distinct isoforms at the IS (20).

Our results demonstrate that PIP5Kβ is recruited into the IS of activated T cells and that this kinase plays a crucial and nonredundant role in regulating lipid raft dynamics.

We found that PIP5Kβ recruitment into the IS depends directly on CD28 signaling, the costimulatory molecule responsible for lipid raft assembly at the T:APC contact zone (14, 44), and does not require lipid kinase activity, as the kinase-dead PIP5Kβ[K138A] mutant was still recruited to the T:APC interface. Previous findings have demonstrated the requirement for the presence of the C-terminal domain for PIP5Kβ targeting within different membrane compartments (36). Consistently, we found that a dominant-negative C-terminal mutant of PIP5Kβ, containing a deletion in the last 83 aa (PIP5KβΔ456), failed to polarize to the T:APC interface following CD28 stimulation. Furthermore, the C-terminal 83-aa tail of PIP5Kβ was essential for regulating F-actin accumulation and remodeling at the IS upon T cell activation. Indeed, the ability of PIP5Kβ to induce actin remodeling is known to depend on kinase activity as well as membrane targeting (28, 31, 45).

Spatiotemporal segregation of signaling molecules has a key role in activating specific downstream responses. In T lymphocytes,

FIGURE 4. The C-terminal domain of PIP5Kβ is required for membrane raft recruitment into the IS and T cell activation. (**A**) JE6.1 Jurkat T cells transfected with EGFP-PIPKβ (white bar) or EGFP-PIP5KβΔ456 (black bar) were allowed to form conjugates with super-antigen (SEE)-pulsed 5-3.1 fibroblasts expressing B7-1 and analyzed for lipid raft recruitment to the IS. Representative confocal images of lipid raft marker myr-palm-CFP (red) to the IS, in the presence of EGFP-PIP5Kβ (green) or EGFP-PIP5KβΔ456 (green) are shown. Yellow coloration indicates overlap of the red and green signals. (**B**) Graph displays the quantitative analysis of lipid raft recruitment to the IS (RRI). Scale bar, 10 μm. Bars show mean RRI values ± SEM from 32 (PIP5Kβ) and 28 (PIP5KβΔ456) conjugates. An unpaired *t* test was performed. ***$p < 0.001$. (**C**) Jurkat cells were transfected with EGFP-PIPKβ or EGFP-PIP5KβΔ456 for 24 h and then stimulated for 15 min with 5-3.1/B7 cells. Conjugate formation was measured by flow cytometry and expressed as the mean percentage ± SEM of two independent experiments performed in quadruplicate. Data are representative of two independent experiments.
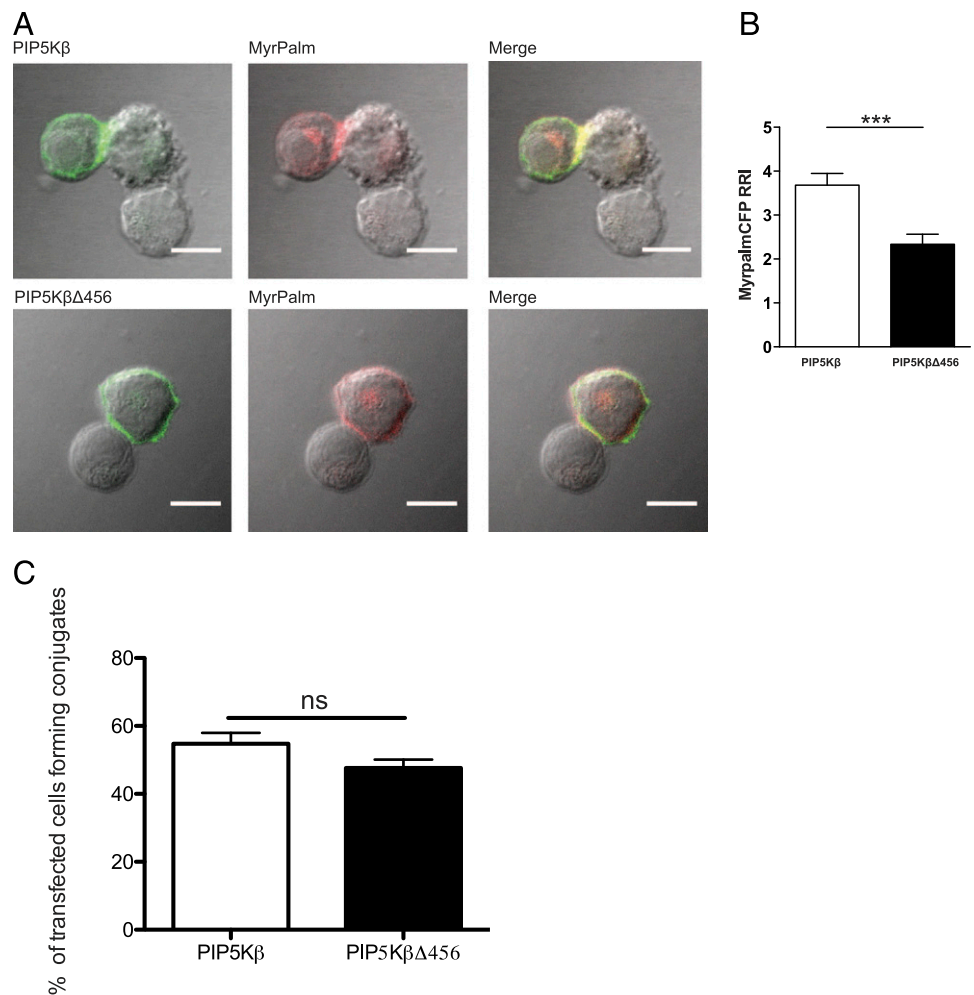
FIGURE 5. PIP5Kβ knockdown impairs TCR- and CD28-dependent activation of T cells. (**A**) Primary human CD4$^+$ T cells were transfected with PIP5Kβ small interfering RNA or scrambled control small interfering RNA. A representative experiment of three independent experiments with identical results is shown. Real-time PCR was used to measure PIP5Kβ mRNA levels 48 h after PIP5Kβ or scrambled control small interfering RNA transfection. (**B**) Fluo-3-AM–loaded T cells, transfected with PIP5Kβ small interfering RNA or scrambled control small interfering RNA, were stimulated for 2 min at 37°C with cross-linked anti-CD3 plus anti-CD28 Abs, and changes in intracellular calcium were detected by flow cytometry analysis. (**C** and **D**) Primary human CD4$^+$ T cells, transfected with PIP5Kβ small interfering RNA or with scrambled control small interfering RNA, were stimulated with anti-CD3 plus anti-CD28 Abs for 12 h, and activation markers CD69 (C) and CD25 (D) were measured by flow cytometry. One-way ANOVA and Tukey's posttests were applied. **$p < 0.01$, ***$p < 0.001$.
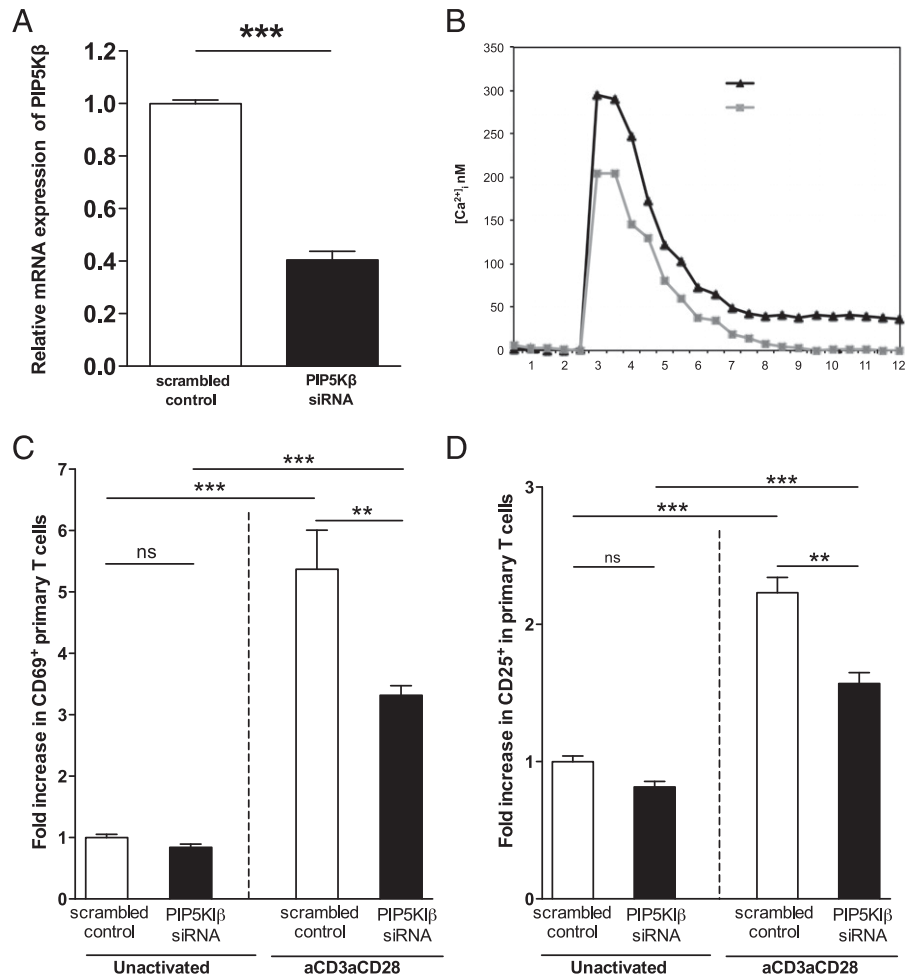
TCR ligation by peptide–MHC complexes on APCs results in the redistribution of the TCR, adhesion molecules, and other crucial signaling mediators to the interface between the two cells. Following T lymphocyte stimulation, membrane lipid rafts cluster at the IS, thus allowing the recruitment of several key regulators of the T signalosome. In addition, several components of the actin-based cytoskeleton, such as ezrin radixin moesin proteins, talin, and vinculin, are selectively concentrated in lipid raft domains (46). CD28 is the crucial determinant of T lymphocyte activation, as it promotes the cytoskeletal rearrangement events required for relocalization of receptors, lipid raft accumulation, and organization of a signaling compartment at the IS (9, 14). CD28 regulates the remodeling of the actin cytoskeleton independently of TCR signals (33, 47, 48), thus acting as an amplifier of both early TCR signaling (10, 12) and autonomous signaling mediator (49, 50). CD28 also recruits FLNA, which in turn cooperates with Vav1 in mediating the actin polymerization pathway to induce lipid raft accumulation at the IS (14). Specialized lipid rafts, rich in glycosphingolipids and cholesterol, within plasma membranes, have been reported to concentrate PIP2, possibly accounting for half of the total PIP2 at the cell surface (16). Raft isolation showed that PIP5K is not enriched in rafts in platelets (51), whereas it is found to be recruited to lipid rafts during B cell activation (32). We found that PIP5Kβ is directly involved in both the recruitment of FLNA and the accumulation of lipid rafts to the IS. Indeed, PIP5KβΔ456 mutant failed to induce both FLNA and lipid raft recruitment to the IS. Moreover, consistently with our previous findings indicating that Vav1 is required for CD28-induced FLNA recruitment into the IS (14), we found a requirement for Vav1 in

CD28-mediated recruitment of PIP5Kβ to the membrane. Our data indicate that PIP5Kβ is critical for Vav1 effector functions, as the overexpression of PIP5KβΔ456 mutant impaired CD28-dependent Vav1 signaling functions. This is also in agreement with the observed cooperation between PIP5Kα and Vav1 in promoting actin polymerization and CD28 signaling functions in human T lymphocytes (22).

Polymerization of actin filaments against cellular membranes provides the force for a variety of cellular processes, by controlling cell shape, endo- and exocytosis, cell migration, and cell–cell adhesion (1). PIP2 accumulates at sites of cell surface motility and can modulate actin dynamics by acting as a platform for protein recruitment, by triggering signaling cascades, and by directly regulating the activities of actin-binding proteins (31, 52, 53). The local accumulation of PIP2-enriched raft domains has a central role in controlling the protrusion dynamics, regulating both signaling pathways, membrane shaping, cell motility, and polarization (15). Interestingly, we found that PIP5Kβ recruitment to the IS affects cytoskeletal rearrangements, as shown by the dominant-negative effects of PIP5Kβ Δ456 on T cell spreading and podia formation upon stimulation. Furthermore, the relevance of PIP5Kβ contribution to efficient T cell activation was demonstrated by the significant impairment of calcium influx as well as CD69 and CD25 upregulation in stimulated PIP5Kβ-silenced primary T cells.

The results presented in this work, together with our previous findings on PIP5Kα relevance in CD28-mediated costimulatory signals (21, 22), suggest that distinct PIP2 pools generated from distinct kinases have functionally unique roles in orchestrating

CD28-mediated actin remodeling in human T lymphocytes. By examining both PIP5Kα and PIP5Kβ localizations and deciphering their important role in the organization of the signaling compartment at the IS, we identified PIP5Kβ as a key molecule that participates in tethering membrane rafts to the actin cytoskeleton during T lymphocyte activation, whereas PIP5Kα ensures the replenishment of the PIP2 pool necessary for the activation of phospholipase Cγ1- and PI3K-regulated downstream signaling pathways (19, 21, 22). Interestingly, Lacalle et al. (54) have recently demonstrated that PIP5Kα/PIP5Kβ dimerization is essential for both membrane localization and PIP2 synthesis. Our findings on the association of Vav1 with both PIP5Kβ and PIP5Kα, together with our previous data that Vav1, but not PIP5Kα, coprecipitated with CD28 following stimulation (22), are thus highly compatible with a model in which, by binding the C-terminal proline-rich motif of CD28 (22), Vav1 is a crucial determinant for the corecruitment to the membrane of PIP5Kβ/ PIP5Kα dimers as well as for their functional activities in response to CD28 stimulation.

Acknowledgments

Disclosures

The authors have no financial conflicts of interest.

References

1. Di Paolo, G., and P. De Camilli. 2006. Phosphoinositides in cell regulation and membrane dynamics. *Nature* 443: 651–657.
2. Kwiatkowska, K. 2010. One lipid, multiple functions: how various pools of PI(4,5)P(2) are created in the plasma membrane. *Cell. Mol. Life Sci.* 67: 3927–3946.
3. Feske, S. 2007. Calcium signalling in lymphocyte activation and disease. *Nat. Rev. Immunol.* 7: 690–702.
4. Kane, L. P., and A. Weiss. 2003. The PI-3 kinase/Akt pathway and T cell activation: pleiotropic pathways downstream of PIP3. *Immunol. Rev.* 192: 7–20.
5. Oude Weernink, P. A., M. Schmidt, and K. H. Jakobs. 2004. Regulation and cellular roles of phosphoinositide 5-kinases. *Eur. J. Pharmacol.* 500: 87–99.
6. Fukami, K., K. Furuhashi, M. Inagaki, T. Endo, S. Hatano, and T. Takenawa. 1992. Requirement of phosphatidylinositol 4,5-bisphosphate for alpha-actinin function. *Nature* 359: 150–152.
7. Gilmore, A. P., and K. Burridge. 1996. Regulation of vinculin binding to talin and actin by phosphatidyl-inositol-4-5-bisphosphate. *Nature* 381: 531–535.
8. Davis, D. M., and M. L. Dustin. 2004. What is the importance of the immunological synapse? *Trends Immunol.* 25: 323–327.
9. Tavano, R., G. Gri, B. Molon, B. Marinari, C. E. Rudd, L. Tuosto, and A. Viola. 2004. CD28 and lipid rafts coordinate recruitment of Lck to the immunological synapse of human T lymphocytes. *J. Immunol.* 173: 5392–5397.
10. Viola, A. 2001. The amplification of TCR signaling by dynamic membrane microdomains. *Trends Immunol.* 22: 322–327.
11. Viola, A., and A. Lanzavecchia. 1996. T cell activation determined by T cell receptor number and tunable thresholds. *Science* 273: 104–106.
12. Tuosto, L., and O. Acuto. 1998. CD28 affects the earliest signaling events generated by TCR engagement. *Eur. J. Immunol.* 28: 2131–2142.
13. Viola, A., S. Schroeder, Y. Sakakibara, and A. Lanzavecchia. 1999. T lymphocyte costimulation mediated by reorganization of membrane microdomains. *Science* 283: 680–682.
14. Tavano, R., R. L. Contento, S. J. Baranda, M. Soligo, L. Tuosto, S. Manes, and A. Viola. 2006. CD28 interaction with filamin-A controls lipid raft accumulation at the T-cell immunological synapse. *Nat. Cell Biol.* 8: 1270–1276.
15. Simons, K., and M. J. Gerl. 2010. Revitalizing membrane rafts: new tools and insights. *Nat. Rev. Mol. Cell Biol.* 11: 688–699.
16. Pike, L. J., and J. M. Miller. 1998. Cholesterol depletion delocalizes phosphatidylinositol bisphosphate and inhibits hormone-stimulated phosphatidylinositol turnover. *J. Biol. Chem.* 273: 22298–22304.
17. Golub, T., and P. Caroni. 2005. PI(4,5)P2-dependent microdomain assemblies capture microtubules to promote and control leading edge motility. *J. Cell Biol.* 169: 151–165.
18. van den Bout, I., and N. Divecha. 2009. PIP5K-driven PtdIns(4,5)P2 synthesis: regulation and cellular functions. *J. Cell Sci.* 122: 3837–3850.
19. Tuosto, L., C. Capuano, M. Muscolini, A. Santoni, and R. Galandrini. 2015. The multifaceted role of PIP2 in leukocyte biology. *Cell. Mol. Life Sci.* 72: 4461–4474.
20. Sun, Y., R. D. Dandekar, Y. S. Mao, H. L. Yin, and C. Wülfing. 2011. Phosphatidylinositol (4,5) bisphosphate controls T cell activation by regulating T cell rigidity and organization. *PLoS One* 6: e27227.
21. Muscolini, M., C. Camperio, C. Capuano, S. Caristi, E. Piccolella, R. Galandrini, and L. Tuosto. 2013. Phosphatidylinositol 4-phosphate 5-kinase α activation critically contributes to CD28-dependent signaling responses. *J. Immunol.* 190: 5279–5286.
22. Muscolini, M., C. Camperio, N. Porciello, S. Caristi, C. Capuano, A. Viola, R. Galandrini, and L. Tuosto. 2015. Phosphatidylinositol 4-phosphate 5-kinase α and Vav1 mutual cooperation in CD28-mediated actin remodeling and signaling functions. *J. Immunol.* 194: 1323–1333.
23. Bolomini-Vittori, M., A. Montresor, C. Giagulli, D. Staunton, B. Rossi, M. Martinello, G. Constantin, and C. Laudanna. 2009. Regulation of conformer-specific activation of the integrin LFA-1 by a chemokine-triggered Rho signaling module. *Nat. Immunol.* 10: 185–194.
24. Honda, A., M. Nogami, T. Yokozeki, M. Yamazaki, H. Nakamura, H. Watanabe, K. Kawamoto, K. Nakayama, A. J. Morris, M. A. Frohman, and Y. Kanaho. 1999. Phosphatidylinositol 4-phosphate 5-kinase alpha is a downstream effector of the small G protein ARF6 in membrane ruffle formation. *Cell* 99: 521–532.
25. Padrón, D., Y. J. Wang, M. Yamamoto, H. Yin, and M. G. Roth. 2003. Phosphatidylinositol phosphate 5-kinase Ibeta recruits AP-2 to the plasma membrane and regulates rates of constitutive endocytosis. *J. Cell Biol.* 162: 693–701.
26. Wong, K. W., and R. R. Isberg. 2003. Arf6 and phosphoinositol-4-phosphate-5-kinase activities permit bypass of the Rac1 requirement for beta1 integrin-mediated bacterial uptake. *J. Exp. Med.* 198: 603–614.
27. Matsui, T., S. Yonemura, S. Tsukita, and S. Tsukita. 1999. Activation of ERM proteins in vivo by Rho involves phosphatidyl-inositol 4-phosphate 5-kinase and not ROCK kinases. *Curr. Biol.* 9: 1259–1262.
28. Shibasaki, Y., H. Ishihara, N. Kizuki, T. Asano, Y. Oka, and Y. Yazaki. 1997. Massive actin polymerization induced by phosphatidylinositol-4-phosphate 5-kinase in vivo. *J. Biol. Chem.* 272: 7578–7581.
29. Tolias, K. F., J. H. Hartwig, H. Ishihara, Y. Shibasaki, L. C. Cantley, and C. L. Carpenter. 2000. Type Ialpha phosphatidylinositol-4-phosphate 5-kinase mediates Rac-dependent actin assembly. *Curr. Biol.* 10: 153–156.
30. Yamamoto, M., D. H. Hilgemann, S. Feng, H. Bito, H. Ishihara, Y. Shibasaki, and H. L. Yin. 2001. Phosphatidylinositol 4,5-bisphosphate induces actin stress-fiber formation and inhibits membrane ruffling in CV1 cells. *J. Cell Biol.* 152: 867–876.
31. Rozelle, A. L., L. M. Machesky, M. Yamamoto, M. H. Driessens, R. H. Insall, M. G. Roth, K. Luby-Phelps, G. Marriott, A. Hall, and H. L. Yin. 2000. Phosphatidylinositol 4,5-bisphosphate induces actin-based movement of raft-enriched vesicles through WASP-Arp2/3. *Curr. Biol.* 10: 311–320.
32. Saito, K., K. F. Tolias, A. Saci, H. B. Koon, L. A. Humphries, A. Scharenberg, D. J. Rawlings, J. P. Kinet, and C. L. Carpenter. 2003. BTK regulates PtdIns-4,5-P2 synthesis: importance for calcium signaling and PI3K activity. *Immunity* 19: 669–678.
33. Piccolella, E., F. Spadaro, C. Ramoni, B. Marinari, A. Costanzo, M. Levrero, L. Thomson, R. T. Abraham, and L. Tuosto. 2003. Vav-1 and the IKK alpha subunit of I kappa B kinase functionally associate to induce NF-kappa B activation in response to CD28 engagement. *J. Immunol.* 170: 2895–2903.
34. Michel, F., G. Mangino, G. Attal-Bonnefoy, L. Tuosto, A. Alcover, A. Roumier, D. Olive, and O. Acuto. 2000. CD28 utilizes Vav-1 to enhance TCR-proximal signaling and NF-AT activation. *J. Immunol.* 165: 3820–3829.
35. Grynkiewicz, G., M. Poenie, and R. Y. Tsien. 1985. A new generation of Ca2+ indicators with greatly improved fluorescence properties. *J. Biol. Chem.* 260: 3440–3450.
36. Lacalle, R. A., R. M. Peregil, J. P. Albar, E. Merino, C. Martínez-A, I. Mérida, and S. Mañes. 2007. Type I phosphatidylinositol 4-phosphate 5-kinase controls neutrophil polarity and directional movement. *J. Cell Biol.* 179: 1539–1553.
37. Itoh, T., H. Ishihara, Y. Shibasaki, Y. Oka, and T. Takenawa. 2000. Autophosphorylation of type I phosphatidylinositol phosphate kinase regulates its lipid kinase activity. *J. Biol. Chem.* 275: 19389–19394.
38. Tybulewicz, V. L. J. 2005. Vav-family proteins in T-cell signalling. *Curr. Opin. Immunol.* 17: 267–274.
39. Stossel, T. P., J. Condeelis, L. Cooley, J. H. Hartwig, A. Noegel, M. Schleicher, and S. S. Shapiro. 2001. Filamins as integrators of cell mechanics and signalling. *Nat. Rev. Mol. Cell Biol.* 2: 138–145.
40. Zhou, A. X., J. H. Hartwig, and L. M. Akyürek. 2010. Filamins in cell signaling, transcription and organ development. *Trends Cell Biol.* 20: 113–123.
41. Hayashi, K., and A. Altman. 2006. Filamin A is required for T cell activation mediated by protein kinase C-theta. *J. Immunol.* 177: 1721–1728.
42. Liu, Y., L. Casey, and L. J. Pike. 1998. Compartmentalization of phosphatidylinositol 4,5-bisphosphate in low-density membrane domains in the absence of caveolin. *Biochem. Biophys. Res. Commun.* 245: 684–690.
43. Singleton, K. L., K. T. Roybal, Y. Sun, G. Fu, N. R. Gascoigne, N. S. van Oers, and C. Wülfing. 2009. Spatiotemporal patterning during T cell activation is highly diverse. *Sci. Signal.* 2: ra15.
44. Viola, A., and N. Gupta. 2007. Tether and trap: regulation of membrane-raft dynamics by actin-binding proteins. *Nat. Rev. Immunol.* 7: 889–896.
45. Ishihara, H., Y. Shibasaki, N. Kizuki, T. Wada, Y. Yazaki, T. Asano, and Y. Oka. 1998. Type I phosphatidylinositol-4-phosphate 5-kinases: cloning of the third isoform and deletion/substitution analysis of members of this novel lipid kinase family. *J. Biol. Chem.* 273: 8741–8748.

46. Pizzo, P., and A. Viola. 2003. Lymphocyte lipid rafts: structure and function. *Curr. Opin. Immunol.* 15: 255–260.
47. Muscolini, M., A. Sajeva, S. Caristi, and L. Tuosto. 2011. A novel association between filamin A and NF-κB inducing kinase couples CD28 to inhibitor of NF-κB kinase α and NF-κB activation. *Immunol. Lett.* 136: 203–212.
48. Salazar-Fontana, L. I., V. Barr, L. E. Samelson, and B. E. Bierer. 2003. CD28 engagement promotes actin polymerization through the activation of the small Rho GTPase Cdc42 in human T cells. *J. Immunol.* 171: 2225–2232.
49. Camperio, C., M. Muscolini, E. Volpe, D. Di Mitri, R. Mechelli, M. C. Buscarinu, S. Ruggieri, E. Piccolella, M. Salvetti, C. Gasperini, et al. 2014. CD28 ligation in the absence of TCR stimulation up-regulates IL-17A and pro-inflammatory cytokines in relapsing-remitting multiple sclerosis T lymphocytes. *Immunol. Lett.* 158: 134–142.
50. Tuosto, L. 2011. NF-κB family of transcription factors: biochemical players of CD28 co-stimulation. *Immunol. Lett.* 135: 1–9.
51. Yang, S. A., C. L. Carpenter, and C. S. Abrams. 2004. Rho and Rho-kinase mediate thrombin-induced phosphatidylinositol 4-phosphate 5-kinase trafficking in platelets. *J. Biol. Chem.* 279: 42331–42336.
52. Botelho, R. J., M. Teruel, R. Dierckman, R. Anderson, A. Wells, J. D. York, T. Meyer, and S. Grinstein. 2000. Localized biphasic changes in phosphatidylinositol-4,5-bisphosphate at sites of phagocytosis. *J. Cell Biol.* 151: 1353–1368.
53. Yin, H. L., and P. A. Janmey. 2003. Phosphoinositide regulation of the actin cytoskeleton. *Annu. Rev. Physiol.* 65: 761–789.
54. Lacalle, R. A., J. C. de Karam, L. Martínez-Muñoz, I. Artetxe, R. M. Peregil, J. Sot, A. M. Rojas, F. M. Goñi, M. Mellado, and S. Mañes. 2015. Type I phosphatidylinositol 4-phosphate 5-kinase homo- and heterodimerization determines its membrane localization and activity. *FASEB J.* 29: 2371–2385.
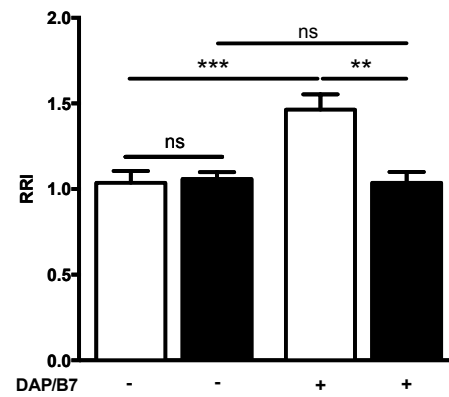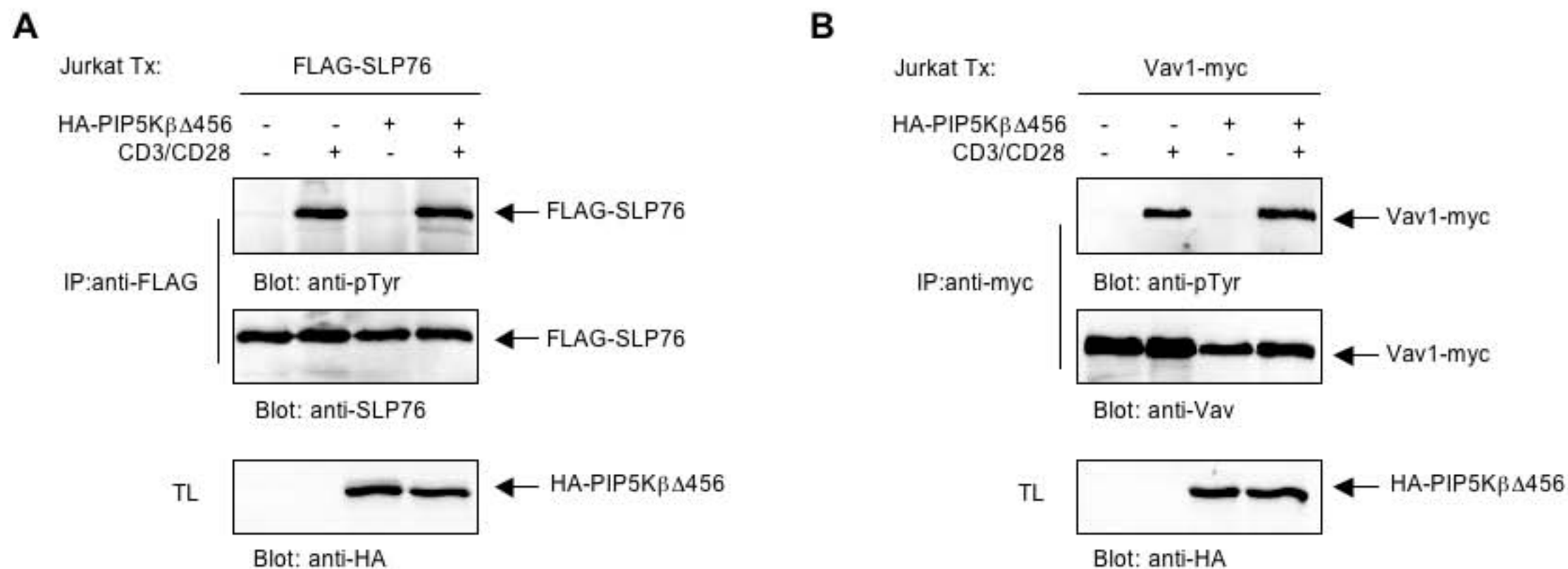
Supplemental Figure 1

Primary human CD4^{+} T cells, transfected with either PIP5Kβ (white bars) or PIP5KβΔ456 (black bars) were incubated with superantigen (sAg) (SEE)-pulsed Dap3 cells, expressing or not human B7-1, for 15 minutes. Quantitative analysis of recruitment (RRI) EGFP-PIP5Kβ to the IS is shown. Non-parametric 1-way ANOVA test was performed; ns: not significant; **: $p < 0.01$; ***: $p < 0.001$
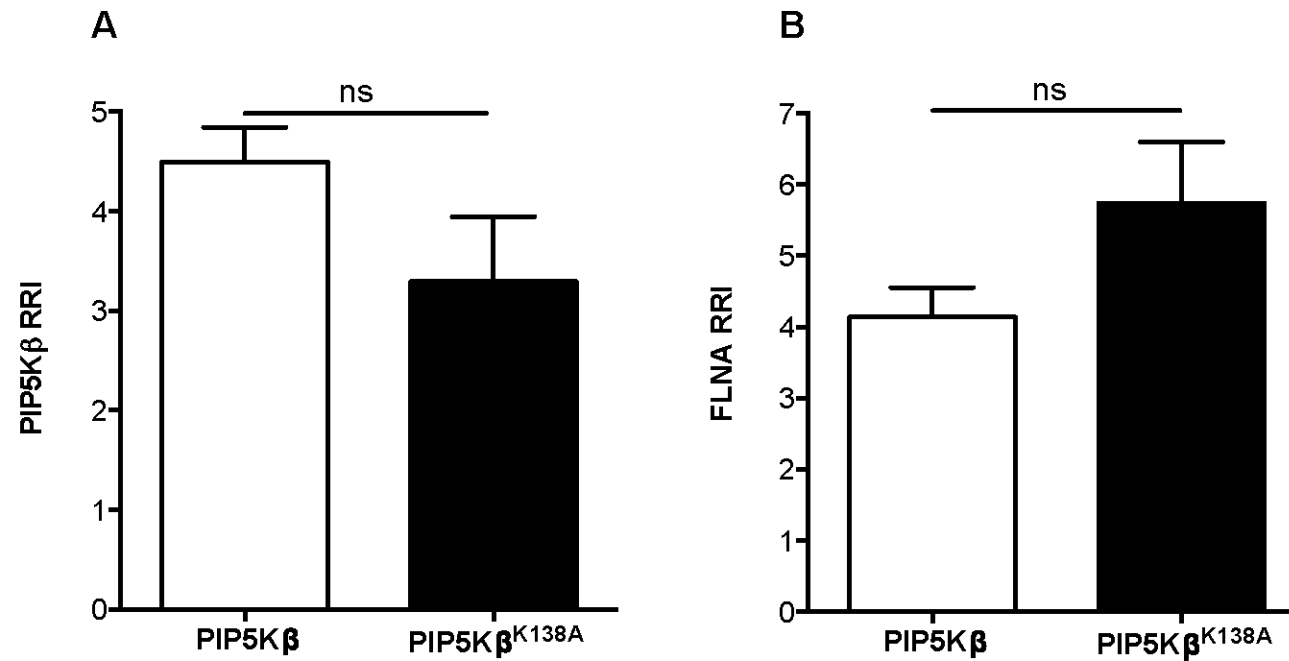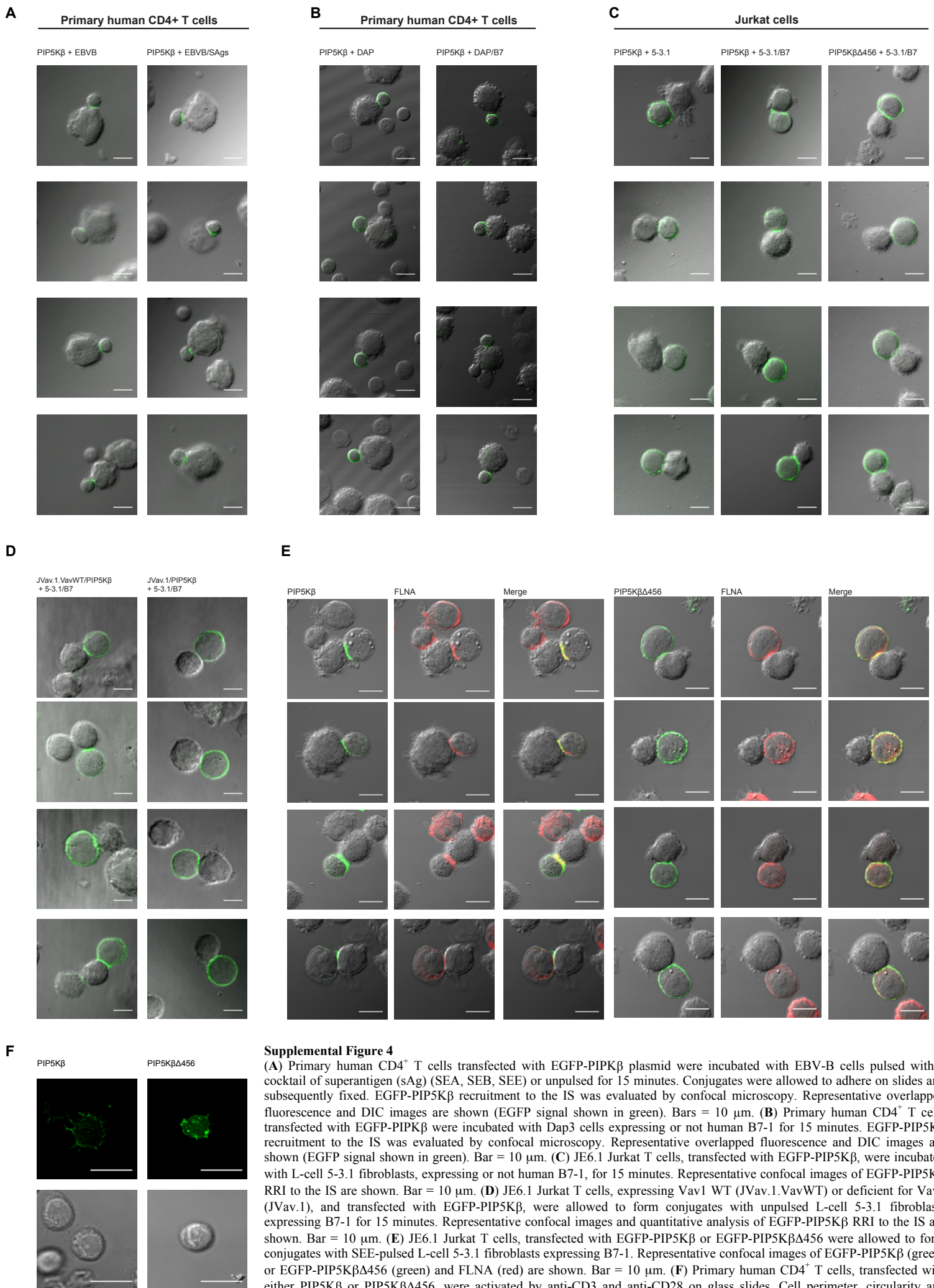
Supplemental Figure 2
JE6.1 Jurkat T cells, transfected with EGFP-PIP5Kβ (white bars) or EGFP-PIP5KβK138A (black bars) were allowed to form conjugates with L-cell 5-3.1 SEE-pulsed fibroblasts expressing B7-1. The graph displays the quantitative analysis of both PIP5Kβ and FLNA recruitment to the IS (RRI). Unpaired T- test was used; ns: not significant. Bar = 10 μm.

Supplemental Figure 3.

PIP5KβΔ456 does not affect early tyrosine phosphorylation events. Jurkat cells were transfected with FLAG-SLP76 (**A**) or Vav1-myc (**B**) constructs alone or in combination with HA-PIP5KβΔ456 construct and then stimulated for 5 min with crosslinked anti-CD3 plus anti-CD28 Abs. Anti-phosphotyrosine (anti-pTyr) western blottings (upper panels) were performed on anti-FLAG (**A**) or anti-myc (**B**) immunoprecipitations (IP). The content of immunoprecipitated proteins was evaluated by anti-SLP76 (**A**) or anti-Vav (**B**) western blottings (middle panels). The content of HA-PIP5KβΔ456 in total lysates (TL) was analysed by anti-HA western blottings (lower panels). The experiment is representative of three.

Supplemental Figure 4

(**A**) Primary human CD4$^+$ T cells transfected with EGFP-PIPKβ plasmid were incubated with EBV-B cells pulsed with a cocktail of superantigen (sAg) (SEA, SEB, SEE) or unpulsed for 15 minutes. Conjugates were allowed to adhere on slides and subsequently fixed. EGFP-PIP5Kβ recruitment to the IS was evaluated by confocal microscopy. Representative overlapped fluorescence and DIC images are shown (EGFP signal shown in green). Bars = 10 μm. (**B**) Primary human CD4$^+$ T cells transfected with EGFP-PIPKβ were incubated with Dap3 cells expressing or not human B7-1 for 15 minutes. EGFP-PIP5Kβ recruitment to the IS was evaluated by confocal microscopy. Representative overlapped fluorescence and DIC images are shown (EGFP signal shown in green). Bar = 10 μm. (**C**) JE6.1 Jurkat T cells, transfected with EGFP-PIP5Kβ, were incubated with L-cell 5-3.1 fibroblasts, expressing or not human B7-1, for 15 minutes. Representative confocal images of EGFP-PIP5Kβ RRI to the IS are shown. Bar = 10 μm. (**D**) JE6.1 Jurkat T cells, expressing Vav1 WT (JVav.1.VavWT) or deficient for Vav1 (JVav.1), and transfected with EGFP-PIP5Kβ, were allowed to form conjugates with unpulsed L-cell 5-3.1 fibroblasts expressing B7-1 for 15 minutes. Representative confocal images and quantitative analysis of EGFP-PIP5Kβ RRI to the IS are shown. Bar = 10 μm. (**E**) JE6.1 Jurkat T cells, transfected with EGFP-PIP5Kβ or EGFP-PIP5KβΔ456 were allowed to form conjugates with SEE-pulsed L-cell 5-3.1 fibroblasts expressing B7-1. Representative confocal images of EGFP-PIP5Kβ (green) or EGFP-PIP5KβΔ456 (green) and FLNA (red) are shown. Bar = 10 μm. (**F**) Primary human CD4$^+$ T cells, transfected with either PIP5Kβ or PIP5KβΔ456, were activated by anti-CD3 and anti-CD28 on glass slides. Cell perimeter, circularity and number of podia was evaluated 1h after activation by confocal analysis. Representative fluorescence and DIC images are shown (fluorescence in green represents PIP5Kβ or PIP5KβΔ456). Bar = 10 μm.